Biocatalysis and Agricultural Biotechnology 20 (2019) 101252

Contents lists available at ScienceDirect

Biocatalysis and Agricultural Biotechnology

journal homepage: www.elsevier.com/locate/bab

Integrated bio-pyro-hydro-metallurgical approach to recover metal values from petroleum refinery spent catalyst

Neha Nagar[a], Himanshi Garg[a], Chandra Sekhar Gahan[a,b,*]

[a] Department of Microbiology, School of Life Sciences, Central University of Rajasthan, NH-8, Bandarsindri, Kishangarh, Ajmer, 305817, Rajasthan, India
[b] Department of Sports Biosciences, School of Sports Sciences, Central University of Rajasthan, NH-8, Bandarsindri, Tehsil Kishangarh, Dist-Ajmer, 305817, Rajasthan, India

ARTICLE INFO

Keywords:
Spent petroleum catalyst
Bioleaching
Roasting
Alkaline leaching
SO_2 emission

ABSTRACT

The present study reports an integrated three-step bio-pyro- hydrometallurgical process to recover nickel (Ni) and molybdenum (Mo) from spent petroleum catalyst. High leaching yields of nickel (94%) and molybdenum (92%) along with other critical metals like rhenium, selenium, niobium, chromium, and zirconium were obtained. A toxic element like Pb was leached entirely from the spent catalyst while precious metal like palladium was concentrated during the treatment. The waste petroleum catalyst and all the residues were characterized to understand the morphology, chemical composition, and mineralogy by Scanning Electron Microscopy-Electron Dispersive X-Ray spectroscopy (SEM-EDAX), X-Ray Fluorescence (XRF) and X-Ray Diffraction (XRD) respectively, while the Ni and Fe concentration in the bioleach liquor was analyzed by Atomic Absorption Spectroscopy (AAS). In the first stage, bioleaching of spent catalyst leached up to 94% Ni and 71% Mo. The rate-limiting step in Ni bioleaching kinetics was calculated to be both chemically as well as diffusion controlled. The Ni bioleaching followed 1st order reaction kinetics. Integrating roasting (1 h) and alkaline leaching (6 h) with the bioleaching process remarkably increased the recovery of Mo by 21%. Roasting of the spent catalyst after bioleaching lessened not only harmful SO_2 emission by 64.95% but also liberated residual Mo by 23% from the aluminium silicate matrix. Therefore, employing a sequential bio-pyro-hydrometallurgical technique is a more eco-friendly and cost-effective strategy to recover metal values from spent petroleum catalyst.

1. Introduction

Petroleum catalysts are utilized in various refining processes to increase the process efficiency by enhancing the quality of the feedstock. The growing requirement of clean quality fuel has hiked the global refining catalyst demand and consumption by 3.6% and 5% per year respectively (Marafi and Rana, 2018, 2017). The poor quality of crude with the presence of metallic impurities and heavy use in the refining process has led to fast deactivation of the catalyst (Marafi and Rana, 2018, 2017). This deactivation is caused due to phase transformation and fouling of active surfaces by metal and coke deposition (Al-Sheeha et al., 2013; Vyas and Ting, 2016). After several cycles of regeneration and reuse, the catalysts are stored in the dumping yard of the refinery. This end of life petroleum refinery catalyst is termed as spent catalyst. Globally, 1.5–1.7 million tons of spent petroleum catalyst is being sent to the dumping yard as hazardous petroleum refinery wastes annually (Marafi and Stanislaus, 2008). Spent catalyst is a potential secondary resource of metals like Ni (0.5–6%), Co (1–6%), Mo (10–30%) and V (1–12%) in the alumina matrix. These spent catalyst are also reservoirs of rare earth mineral complexes of lanthanum oxide (~2%), cerium oxide (~2.16%) along with precious metals (Pd, Pt, Rh, etc.) (Akcil et al., 2015; Ding et al., 2019; Wang et al., 2017). Therefore, the utilization of spent catalyst for metal recovery would cater to the demand for critical metals in alloy manufacturing and overcome the environmental and landfilling issues.

Pyrometallurgy and Hydrometallurgy are the two major metallurgical processes followed today for metal extraction from spent petroleum catalyst. The hydrometallurgical approach employs strong acid (H_2SO_4, HCl) or strong base (NaOH, Na_2CO_3, NH_4OH, NH_4Cl, $(NH_4)_2CO_3$,$NH_3{\cdot}H_2O$) either individually or in combination with oxidants (H_2O_2, $KMnO_4$, etc.) (Al-Sheeha et al., 2013; Marafi and Rana, 2017; Marafi and Stanislaus, 2008; Srichandan et al., 2015; Zhao et al., 2015). Several Pyro-metallurgical approaches such as smelting, calcination and anhydrous chlorination have been applied for metal

* Corresponding author. Department of Microbiology, School of Life Sciences, Central University of Rajasthan, NH-8, Bandarsindri, Kishangarh, Ajmer, 305817, Rajasthan, India.
E-mail address: csgahan_mbio@curaj.ac.in (C.S. Gahan).

https://doi.org/10.1016/j.bcab.2019.101252
Received 6 March 2019; Received in revised form 10 April 2019; Accepted 16 July 2019
Available online 17 July 2019
1878-8181/

extraction from petroleum spent catalyst (Al-Sheeha et al., 2013; Marafi and Rana, 2017; Srichandan et al., 2015). Combining hydro- and pyro-metallurgical processing of spent catalyst by roasting at 700 °C with Na_2CO_3 followed by leaching resulted with good recovery of Mo and V (Marafi and Stanislaus, 2011). Reports also suggest enhanced recovery of Mo by roasting (300–600 °C) followed by alkaline leaching (Al-Sheeha et al., 2013; Marafi and Rana, 2018). Hydro-metallurgical operations need a large amount of chemicals (acids/alkali) and have handling problems together with careful selection of reactor material. Pyro-metallurgical processing is energy intensive along with SO_2 emissions to the atmosphere followed by acid rain. Both hydro- and pyrometallurgical processes may be neither economical nor environmental friendly (Pradhan et al., 2009). Therefore, Bio-hydro-metallurgical processing has emerged to be a much more cost-effective and eco-friendly method for processing of secondary metal resources. Chemolithotrophic Fe- and S- oxidizing acidophiles microorganisms like *Acidithiobacillus thiooxidans* and *Acidithiobacillus ferrooxidans* has been used extensively for biohydrometallurgical applications. It has been observed that ferric ion produced by microbial oxidation of ferrous iron and the protons produced from reduced sulphur oxidation are responsible for the oxidation of metal sulfides and metal oxide respectively. This oxidation of sulfide/oxide minerals from spent catalyst results with the mobilization of metal values into solution.

Previous studies on bioleaching of spent catalyst have proved efficient dissolution of 80–90% nickel with or without decoking and low recovery of molybdenum (Pathak et al., 2014; Pradhan et al., 2013, 2010; Srichandan et al., 2015; Vyas and Ting, 2016). The reasons reported for the lower yield of molybdenum was due to limited solubility of Mo oxo-anions in an acidic solution. Refractory nature of MoS_2 and formation of product layer on the Mo species resists the proton attack on the molecular orbital structure (Kim et al., 2010; Mishra et al., 2007; Pradhan et al., 2010; Sand et al., 2001; Srichandan et al., 2015; Vyas and Ting, 2016). As the bioleaching process is a metal selective approach, two-step leaching strategies were adopted targeting Mo recovery due to the higher solubility of Mo as MoO_4^{2-} in alkaline pH (Pradhan et al., 2013; Srichandan et al., 2015; Vyas and Ting, 2016). Moreover, alkaline solutions are advantageous over acidic solutions due to their high selectivity, direct precipitation of the leached metals and direct wastes discharge (HE et al., 2007; Longa et al., 2014). The present study provides a three-step treatment of the spent catalyst, involving an integrated approach of three-step bioleaching of sulfide mineral matrix followed by a pyrometallurgical step of roasting to burn the organic carbon liberating the metal complexes for hydrometallurgical approach by alkali leaching of metals. The bioleaching was carried out by a mixed culture of acidophilic chemolithotrophic iron and sulphur-oxidizing microorganisms. The pyrometallurgical processing was carried out by roasting at 700 °C burning all coke material present in the bioleached residue liberating metals like Mo entrapped in the organic complex. The hydrometallurgical processing by carbonate and bicarbonate leaching was targeted for liberated metals like Mo and V from the roasted bioleach residues. The metal sulfide oxidation by bioleaching step was employed first to mobilize metals and sulphur species into solution. The resulting bioleach residue contains marginal sulphur, so during the pyrometallurgy process, SO_2 emission (causes environmental pollution and acid rain) could be diminished. Hydro-metallurgical alkali leaching was employed to selective leaching of metals that were not leached by proton and ferric oxidation via bioleaching.

2. Materials and methods

2.1. Petroleum refinery spent catalyst

The petroleum refinery spent catalyst sample was obtained from Indian Oil Corporation Limited (IOCL), Mathura refinery, Uttar Pradesh, India. The crushing and grinding of spent catalyst were achieved by rod milling followed by sieving to a particle size with 80% passing (d_{80}) below 100 μm size fraction. The ground samples were further mixed and divided by coning and quartering method to ensure homogeneity of the feed sample in all bio-pyro-hydro-metallurgical processing.

2.2. Microorganisms and media

The microbial culture for bioleaching was obtained from Lulea University of Technology, Lulea, Sweden. The microbial culture used in the bioleaching experiment was a mixed culture of iron and sulphur-oxidizing microorganism together with archaeal species as revealed from the Q-PCR analysis conducted at Bioclear B·V., Netherlands. The microbial culture dominated with *Acidithiobacillus ferroxidans* (Fe & S - oxidizer), *Leptospirillum ferriphilum* (Fe-oxidizer)followed *by Acidithiobacillus caldus* (S-oxidizer), and *Acidithiobacillus thiooxidans* (S-oxidizer), *Sulphobacillus* sp. (Fe-oxidizer) and *Ferroplasma* (archaeal species, Fe-oxidizer).Microbial culture was grown and repeatedly sub-cultured 0 K medium [$(NH_4)_2SO_4$, 3.0 g/L; KCl, 0.1 g/L; K_2HPO_4, 0.5 g/L; $MgSO_4{\cdot}7H_2O$, 0.5 g/L; $Ca(NO_3)_2{\cdot}4H_2O$, 0.01 g/L] (Silverman and Lundgren, 1959) supplemented with 4.5 g/L of ferrous iron and 2 mM of potassium tetrathionate. The culture was grown at mesophilic temperature (30–35 °C)in acidic pH (Franzmann et al., 2005) on a 2 L batch bioreactor with an agitation rate of 220 rpm. The pH of the growth medium was maintained between pH 1 to pH 2 providing a conducive environment for microbial growth (Plumb et al., 2008; Tan et al., 1998) together with preventing iron precipitation and jarosite formation (Kinnunen and Puhakka, 2005; Leahy and Schwarz, 2009).

2.3. Bioleaching experiment

Batch bioleaching of spent petroleum catalyst was carried out on a 2 L bioreactor. The pulp density of the experiment was 10% (w/v) with a working volume of 1L at 30-35°C temperature. The pH in the reaction was controlled to 1.5 by external addition of acid. The mineral salt growth medium used in the study was 80% (v/v) was iron free (Silverman and Lundgren, 1959). The inoculum used in the experiment was 20% (v/v) comprising of a mixed culture of Fe and S oxidizing microorganisms. The microbial population in the feed culture was 4.96×10^8 cells/ml, with a redox potential value of ~700 mV. An overhead stirrer ensured homogeneous mixing of the pulp with an impeller speed of 220 rpm. A hotplate was placed below the reactor for maintaining temperature with regular measurements of pH and Redox potential in the solution. The increase in pH was maintained at 1.5 by adding 2M/5M H_2SO_4. The total amount of 2M/5M H_2SO_4 was calculated in terms of Kg concentrated H_2SO_4/ton of spent catalyst. The measurement of Redox potential (Rivera Eutech ORP meter) with a platinum electrode against Ag/AgCl reference electrode was done at regular time intervals to monitor the redox activity. Microbial growth was analyzed by the viable cell counting using a bright field microscope with the 10X eyepiece and 100x objectives on an improved Neubauer hemocytometer. Ferrous iron estimation was done by titrimetric method using 1, 10 phenanthroline indicator against cerium sulfate (Sundkvist et al., 2008). The Fe (Total) concentration of the bioleaching solution was measured by two different methods, one by AAS analysis and the other by colorimetric method. The colorimetric method was done on a visible spectrophotometer at 510 nm using ammonium acetate as buffer and 1, 10-phenanthroline as indicator and the solution was saturated with hydroxylamine hydrochloride. Two different methods for total iron estimation was employed to cross check the results. The Ferric concentration was calculated by subtracting concentration of Ferrous from the total Fe. The sulfate ion concentration was determined by turbidimetric method by forming barium sulfate colloidal precipitates on the addition of barium chloride to the diluted samples; recording their absorbance at 420 nm (Kolmert et al., 2000). Nickel (Ni) content in bioleaching solution was measured on regular

Table 1
Elemental composition of Petroleum refinery spent catalyst.

Feed Material (Petroleum refinery spent catalyst)	% (w/w)											
	Al	Mo	S	Ni	P	Si	Fe	K	Ca	Ti	Re	Cr
	43.8	32.0	11.0	5.2	3.6	2.3	0.98	0.5	0.37	0.19	0.099	0.036
	Cu	**Se**	**Ga**	**Zr**	**Rb**	**Sr**	**Pd**	**Nb**	**As**	**Pb**	**Na**	
	0.021	0.017	0.013	0.008	0.006	0.006	ND	ND	ND	ND	ND	

time intervals by AAS (Thermo Scientific-iCE 3000 series). The regular addition of deionized water compensated the water loss due to evaporation during the study. After completion, S/L (solid/liquid) separation was done. The amount of bioleached liquor was also measured and analyzed for Ni concentration by AAS. The residue obtained was thoroughly washed with a measured volume of 1.5 pH water (acidified by 5M H_2SO_4) to avoid precipitation of remaining metal ions in the bioleached residue. The residue was oven dried at 50 °C until no change in weight was observed. The weight loss percentages were calculated.

The bioleached residue was crushed and ground thoroughly before sending for chemical analysis. The morphological and elemental analysis of the feed, as well as residues, was performed with SEM- EDAX (Nova Nano FESEM 450 (FEI)). The major, minor and trace elements along with their mass (%) were confirmed by XRF (Bruker). XRD (Rigaku) was done for the mineralogical study of the bioleached residue by measuring the diffraction patterns at angles between 5° to 90° and step size 0.02 angle/sec using Cu Kα (λ = 1.540598) as an X-Ray source.

The metal recovery or leaching yield was calculated from the elemental analysis of feed and bioleach residues of all batch experiments (Tables 3 and 4) considering the feed weight and bioleach residue weight (Table 5) using the following formulas (Equations 1-3)-

$$M_f = M\%{*}w_f \tag{1}$$

$$M_{br} = M\%{*}w_{br} \tag{2}$$

$$L_Y\ (\%) = \left(1 - \frac{M_{br}}{M_f}\right){*}100 \tag{3}$$

M_f = metal content in the feed;M_{br} = metal content in bioleached residue; $M\%$ = Metal percentage; w_f = weight of feed; w_{br} = weight of bioleached residue; $L_Y(\%)$ = Percentage Leaching Yield.

2.4. Roasting

The bioleached residue was roasted in air environment using 400 ml silica crucibles on a muffle furnace at 700°C for 1 h. The roasted sample was ground on a mortar and pestle for homogeneity prior to XRF analysis for their elemental composition followed by mineralogical analysis by XRD and SEM-EDAX analysis.

2.5. Alkaline leaching

Alkaline leaching was done in a chemical reactor at a working volume of 100 ml. The roasted bioleached residue (10 g) was chemically treated with an alkaline mixture containing 40 g/L carbonate (70.65 g Na_2CO_3) and 20 g/L bicarbonate (27.54 g $NaHCO_3$). Homogenous mixing of the pulp was achieved by using a propeller stirrer made of stainless steel at a stirring speed of 320 rpm. The working temperature was maintained at 70 °C by placing a hot plate below the reactor. To ensure proper working volume, de-ionized water was added at various intervals of the leaching period to compensate the evaporation and maintain a uniform concentration of the leaching reagent. The duration of this batch experiment was 6 h. After completion, the experiment was harvested and filtered for solid-liquid separation. The leach residue obtained as a filter cake was thoroughly washed using deionized water and dried in hot air oven at 60-70 °C until no change in weight was observed followed by grinding using mortar and pestle before the morphological analysis by SEM-EDAX, chemical analysis by XRF and mineralogical analysis by X-Ray diffraction. The leaching yield % was calculated as follows (equations (4)–(6))-

$$M_{rbr} = M\%{*}w_{rbr} \tag{4}$$

$$M_{alr} = M\%{*}w_{alr} \tag{5}$$

$$L_Y\ (\%) = \left(1 - \frac{M_{alr}}{M_{rbr}}\right){*}100 \tag{6}$$

M_{rbr} = metal content in roasted bioleached residue; $M_{alr=}$ metal content in the alkaline leached residue;$M\%$ = Metal percentage; w_{rbr} = weight of roasted bioleach residue; f_{alr} = weight of alkaline leached residue; $L_Y(\%)$ = Percentage Leaching Yield.

3. Result and discussion

3.1. Characterization of spent petroleum catalyst

The analysis of elemental composition and their mass (%) in feed by X-Ray Fluorescence analyzer (XRF) showed the presence of aluminium (43.8%), molybdenum (32%), sulphur (11%), and nickel (5.16%) as major elements and phosphorous (3.59%) along with silica (2.25%) as minor constituents whereas iron (0.981%), potassium (0.491%), calcium (0.371%), chromium (0.0362%) and copper (0.0212%), titanium (0.19%), zirconium (0.008%), rhenium (0.099%), strontium (0.0057%), rubidium (0.0061%), selenium (0.017%) and gallium (0.0126%)are present in trace (Table 1).The mineralogical study revealed the presence of phases viz. aluminium oxide (Al_2O_3), aluminium silicate (Al_2SiO_5), molybdenum oxide ($MoO_2/Mo_{2\cdot25}O_{0\cdot7}$), iron molybdenum Oxide ($MoFeO_4$), molybdenum sulfide (Mo_2S_3), nickel sulfide ($Ni_{3\text{-}x}S_2$) and copper-iron sulfide ($CuFe_2S_3$) (Fig. 1). Scanning Electron Microscopy and Electron Dispersive Spectroscopy (EDS) was done to trace out the arrangements of different elements and their complexes in the feed material (Figs. 2 and 3). Fig. 2 reveals that the scattered pattern of nickel (Ni) match with that of sulphur (S) and oxygen (O) suggesting that Ni is present in both sulphidic and oxidic phases. The similar dotted arrangement was observed in molybdenum (Mo) indicating the presence of molybdenum sulfides and oxides which are also observed in the mineral phases revealed by XRD.

3.2. Bioleaching of spent petroleum refinery catalyst

Bioleaching study was conducted for six days until maximum Ni was leached out in the solution. The main aim of the bioleaching study was to investigate the leaching behavior of metals present in the spent catalyst with a primary focus on Ni. The XRD and EDAX mapping revealed that Ni and Mo both are present in the oxidic and sulphidic phases (Figs. 1–3). Therefore, iron and sulphur-oxidizing mixed consortia were employed for the bioleaching of spent catalyst. The bio-oxidized ferric ion and proton are lixiviant in bioleaching. The ferrous-ferric bio-oxidation and reduction continues until all the metal sulfide is dissolved into the solution (Equation (7)). The pH increased by ferrous bio-oxidation is compensated by the proton produced during sulphur oxidation by sulphur-oxidizing microbes (equation (8) and (9)).

$$MeS + 2Fe^{3+} + 1.5O_2 + H_2O \rightarrow Me^{2+} + 2Fe^{2+} + SO_4{}^{2-} + 2H^+ \tag{7}$$

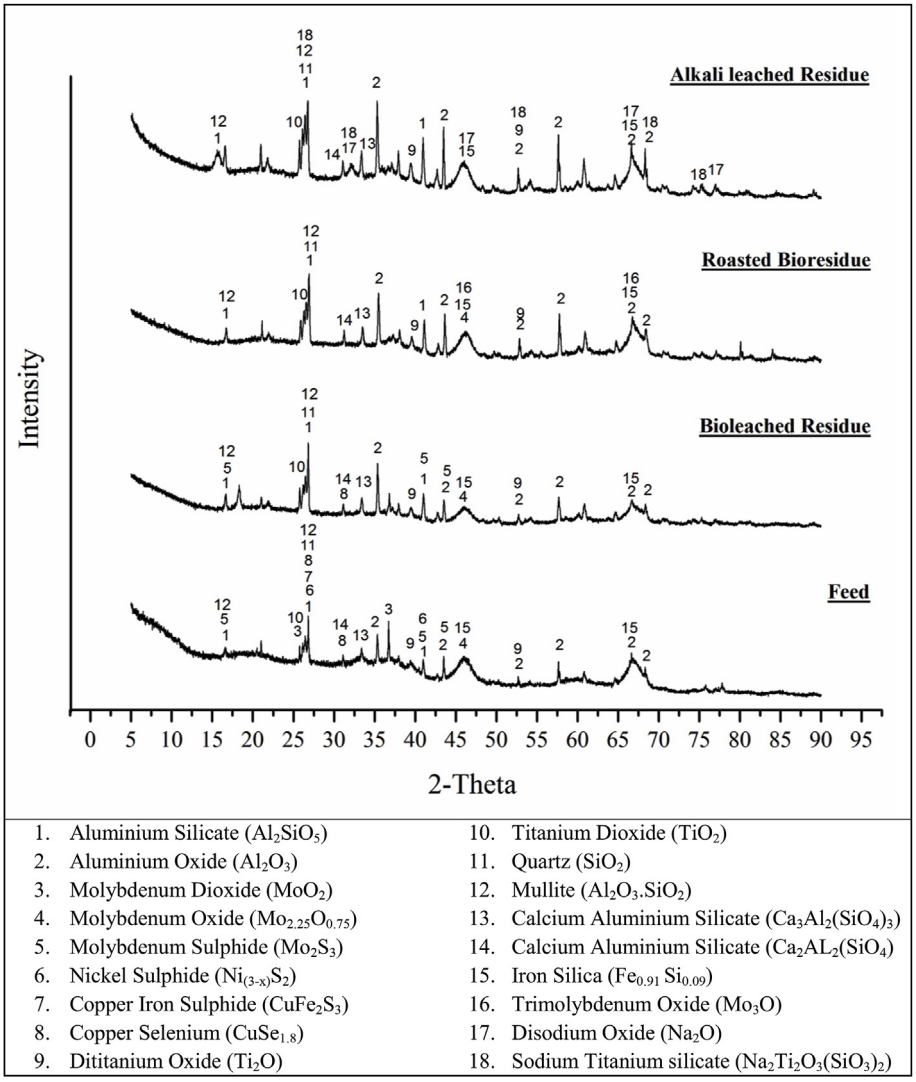

1. Aluminium Silicate (Al_2SiO_5)
2. Aluminium Oxide (Al_2O_3)
3. Molybdenum Dioxide (MoO_2)
4. Molybdenum Oxide ($Mo_{2.25}O_{0.75}$)
5. Molybdenum Sulphide (Mo_2S_3)
6. Nickel Sulphide ($Ni_{(3-x)}S_2$)
7. Copper Iron Sulphide ($CuFe_2S_3$)
8. Copper Selenium ($CuSe_{1.8}$)
9. Dititanium Oxide (Ti_2O)
10. Titanium Dioxide (TiO_2)
11. Quartz (SiO_2)
12. Mullite ($Al_2O_3.SiO_2$)
13. Calcium Aluminium Silicate ($Ca_3Al_2(SiO_4)_3$)
14. Calcium Aluminium Silicate ($Ca_2AL_2(SiO_4)$)
15. Iron Silica ($Fe_{0.91}Si_{0.09}$)
16. Trimolybdenum Oxide (Mo_3O)
17. Disodium Oxide (Na_2O)
18. Sodium Titanium silicate ($Na_2Ti_2O_3(SiO_3)_2$)

Fig. 1. XRD Diffractogram of feed, bioleach residue, roasted bioleach residue and alkaline leached residue.

$$Fe^{2+} + 1/4O_2 + H^+ \rightarrow Fe^{3+} + \tfrac{1}{2} H_2O \quad (8)$$

$$S^0 + 1.5O_2 + H_2O \rightarrow 2H^+ + SO_4^{2-} \quad (9)$$

Apart from the biogenic protons, the pH of the system was maintained at 1.5 by adding 5M H_2SO_4. The pH increased just after feed addition due to the presence of metal oxides (Equation (10)) which consume a lot of acid was maintained at 1.5 by adding 5M H_2SO_4(Fig. 4).

$$MeO + H_2SO_4 \rightarrow MeSO_4 + H_2O \quad (10)$$

It is important to mention here that 38.03% Ni was leached out into the solution just after the feed was added, i.e., before acid addition or at 0 h. Just after bulk acid addition ~4 g H_2SO_4 (8.2 ml 5M H_2SO_4) sample for Ni estimation was again withdrawn quickly. Interestingly, after acid addition, Ni dissolution was increased by 0.78% only (Fig. 5). It indicates that the sufficient concentration of lixiviants, i.e., biogenic proton and ferric ion in the bioleaching medium was responsible for the active dissolution of Ni (38%) and not the externally added 5M H_2SO_4. After 1 h of the experiment, the acid was being consumed by the gangue minerals, but the Ni dissolution (%) was the same. The amount of acid consumption decreased gradually after the first day with the increase in Ni dissolution signifying the role of bacteria and efficacy of the bioleaching process. The total amount of acid consumed was 212 Kg H_2SO_4/ton of spent catalyst (Table 5). The total iron available, i.e., from inoculum and feed, for ferric leaching, was 0.8–1 g/L. It is noteworthy that no external ferrous source was fed to the bacteria. The good ferrous ferric couple was maintained throughout the experiment (Fig. 6). XRD graph of bioleached residue showed no peaks of jarosite signifying little or no precipitation (Fig. 1). The redox potential was in the range of 320–375 mV (Fig. 6). The viable cell count during the experiment was also high i.e., ~3×10^7 cells/ml (Fig. 7). The total amount of sulfate contributed by sulfate compounds in the media and acid (5M H_2SO_4) was calculated to be 32.17 g/L, therefore according to sulfate profile remaining sulfate is supposed to be contributed by sulphur-oxidizing microorganisms in the bioleaching system (Fig. 8). All the above bioleaching conditions favored efficient leaching of nickel and molybdenum, aluminium and other metals to some extent. Mineralogical and chemical analysis by XRF and AAS confirms that nickel was dissolved up to 94% by residue analysis and 91.6% by liquor analysis, i.e., a good mass balance (± 2.4%) was obtained (Tables 1 and 2 and Figs. 1, 5 and 9). The % weight loss in the spent catalyst after bioleaching was 32.67% showing the good dissolution of metal oxides and sulfides by the bacterial attack (Table 5). SEM micrographs show a visible change in the morphology of spent catalyst after bioleaching (Fig. 10A and B). According to the XRF analysis, the oxidic and sulphidic phases of molybdenum accessible to the proton and ferric attack were leached up to 71%. Apart from this, 64.97% of rhenium, 58.71% copper, 30% aluminium, 29.29% phosphorous, 14.08% selenium and

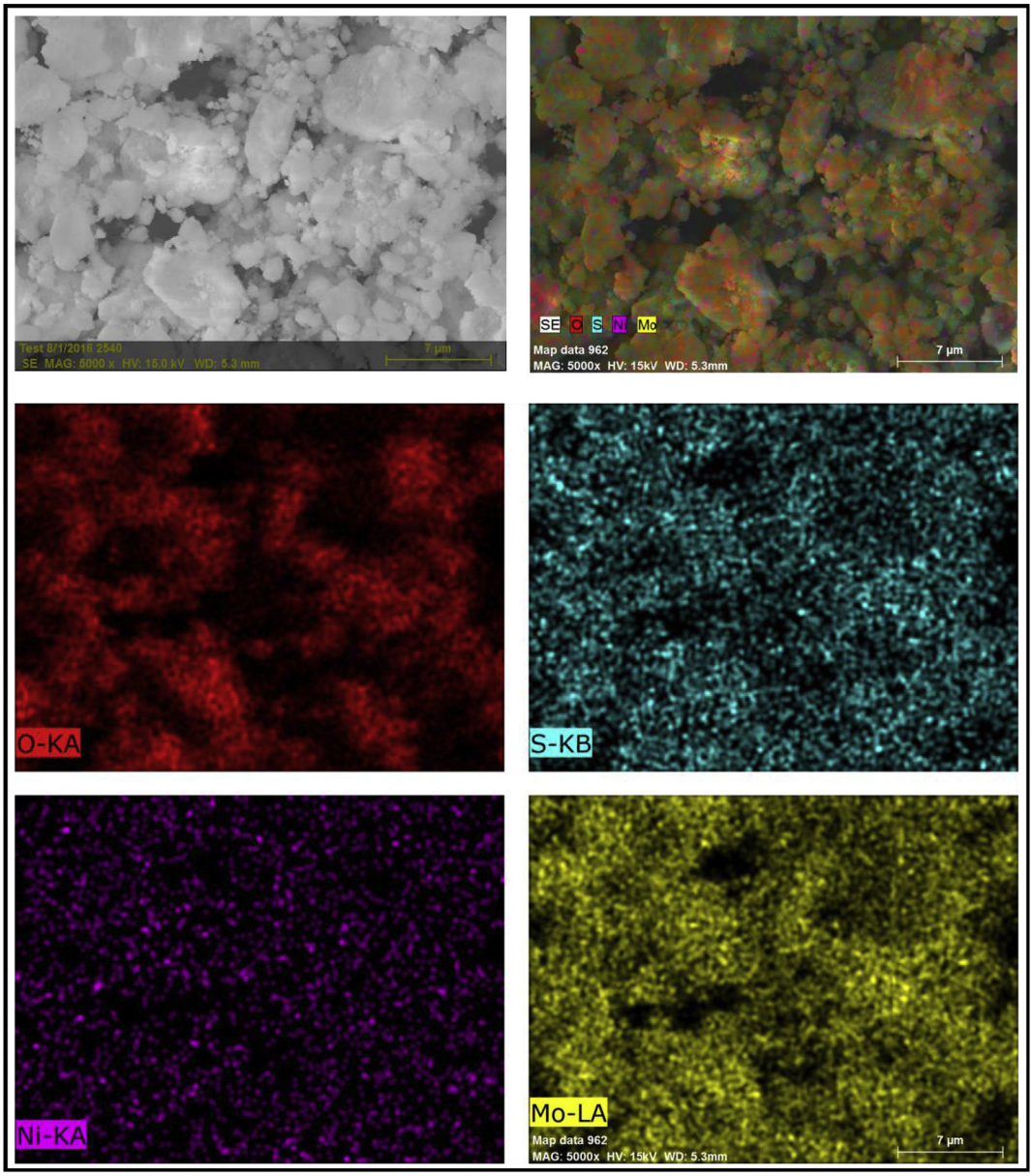

Fig. 2. SEM Micrograph of feed and EDX analysis mapping profiles (point scan) showing selective elements.

8% gallium were leached into the solution (Fig. 9). Chromium (0.03 g in feed) was not detected in the bioleached residue. Several elements such as silica, iron, potassium, calcium, titanium, and zirconium got highly concentrated during bioleaching. Rubidium, strontium, and niobium were concentrated by 67%, 51%, and 1% respectively. Around 19% of palladium was also concentrated. Arsenic which was below the detection limit of XRF in the feed was found to be 0.01 g in the bioleached residue.

3.2.1. Nickel leaching kinetics and determination of rate controlling step

The heterogeneous reaction kinetics of nickel dissolution was examined using shrinking core and shrinking particle models. Evaluation of the rate determining step in the leaching mechanism was carried out by the steps involved in the solid-liquid reaction (Levenspiel, 1999). The diffusion of the lixiviant from the bulk solution to the solid may not be the rate-determining step because leaching was carried out under dynamic conditions (Pradhan et al., 2013). The leaching reaction may also not be limited by product diffusion through product layer and product diffusion into bulk solutions, since product diffusion is expected to be a fast process (Kim et al., 2010). Therefore, the rate-limiting step could only be determined by evaluating the penetration and diffusion through product layer and the chemical reaction between lixiviant and solid. In shrinking particle model, the penetration and diffusion through product layer i.e., resistance in leaching through product layer diffusion is omitted due to no product layer formation. The quantity of reacting lixiviant is proportional to the unreacted surface of the solid core. But, the chemical reaction at the solid surface is slower than diffusion. Thus, the chemical reaction between lixiviant and solid is evaluated for the rate-determining step using Eq. 11

$$\left(\frac{kC}{r_o\rho}\right)t = 1 - (1-\alpha)^{\frac{1}{3}} \tag{11}$$

Where, α = fraction of Ni leached into the solution, t = time, k = rate constant, r_o = original radius of the solid particle, C = concentration of the leach solution, ρ = Density.

Assuming C, ρ, r_o to be constant, rate constant (k) can be calculated by plotting right-hand side of equation (11) with time (t) (Fig. 11). In the shrinking core model, the reaction is controlled by the formation of

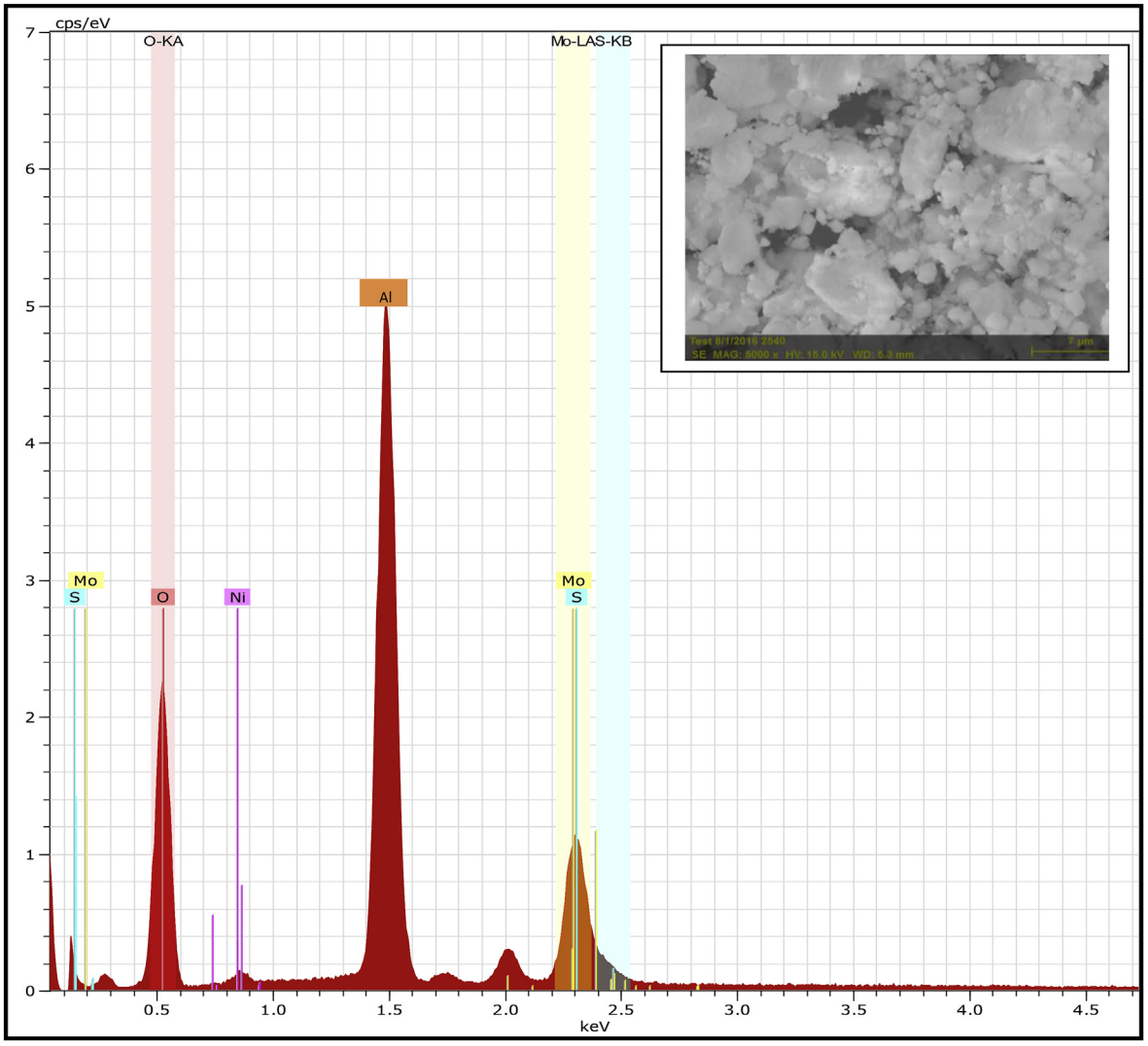

Fig. 3. SEM-EDS micrograph (point scan) of spent catalyst showing its selective elemental contents.

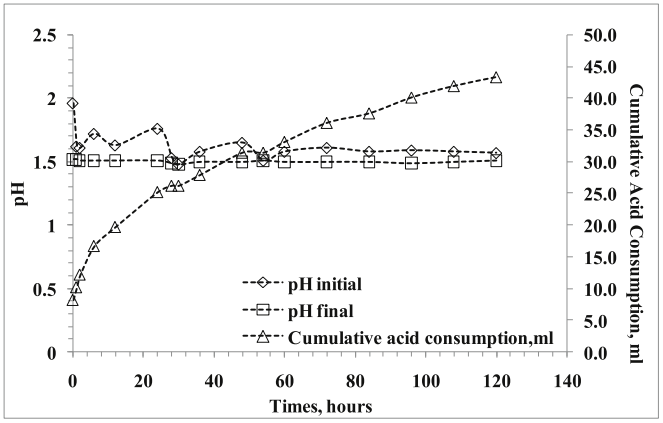

Fig. 4. pH trend during bioleaching of spent catalyst.

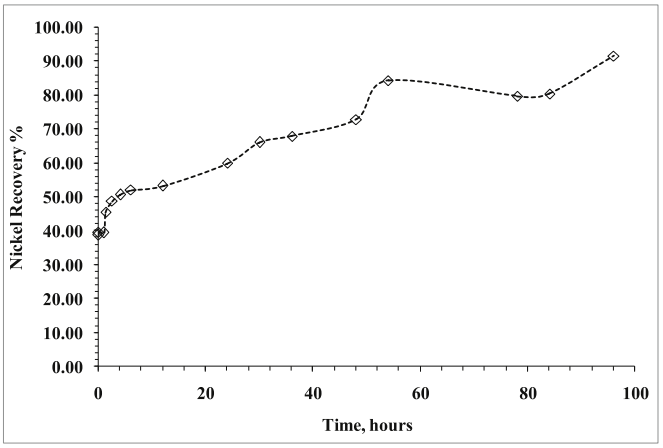

Fig. 5. % Nickel leached in the solution with time.

a product diffusion layer. The chemical reaction at the solid surface is faster than the diffusion. Thus, the penetration and diffusion through product layer is evaluated for the rate-determining step using Eq. (12).

$$\left(\frac{2MDC}{r_o^2\rho\beta}\right)t = 1 - \left(\frac{2}{3}\right)\alpha - (1-\alpha)^{\frac{2}{3}} \quad (12)$$

Where, α = fraction of Ni leached into the solution, t = time, r_o = original radius of the solid particle, M = molecular weight, D = Diffusion constant, C = concentration of the leach solution, ρ = Density, β = stoichiometric factor. Similarly, assuming M, C, ρ, β to be constant, Diffusion constant (D) can be determined by plotting right-hand side of equation (12) against time (t) (Fig. 11). It was observed

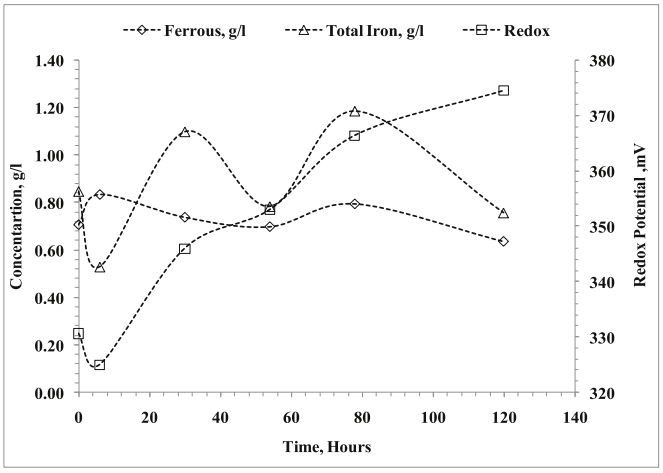

Fig. 6. Ferrous ion concentration and redox potential profiles of the bioleaching experiment.

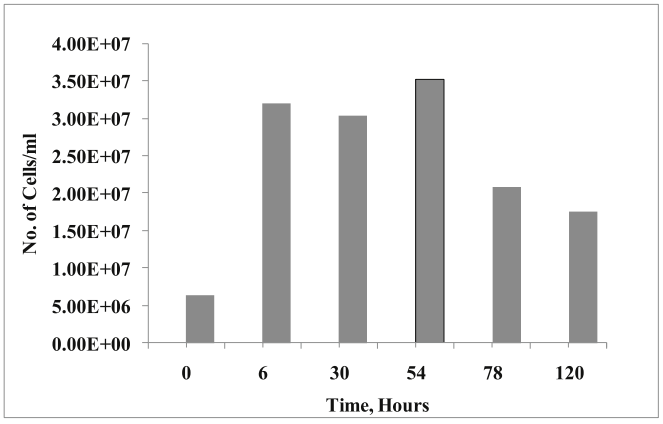

Fig. 7. Viable planktonic cell count profile of the bioleaching experiment.

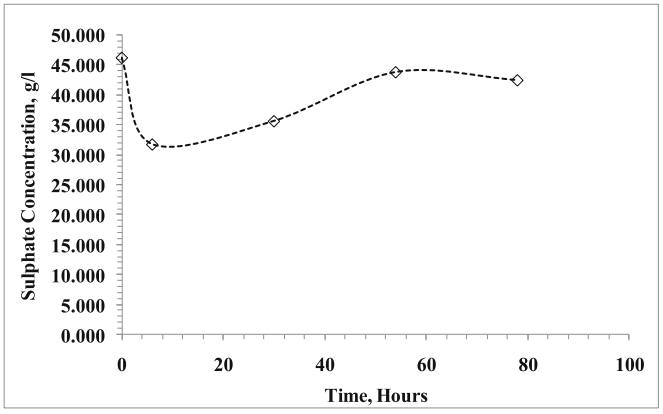

Fig. 8. Sulfate concentration profile of the bioleaching experiment.

that diffusion controlled leaching kinetics was followed by Ni bioleaching. Diffusion controlled model provided a good fit for nickel leaching with Correlation Co-efficient (R^2) 0.9006 and 0.89 respectively (Fig. 10). Therefore, nickel dissolution mechanism is justified by shrinking core model where leaching kinetics is controlled by a non-porous product/passivation layer which hindered the oxidants' diffusion to the mineral surface. The rate constant for chemically controlled leaching mechanism was observed to be 0.0036 and diffusion constant for diffusion controlled leaching kinetics was found to be 0.0016.

3.2.2. Reaction rate and order of reaction

The nickel leaching reaction was evaluated for 1st order or 2nd order reaction kinetics. For 1st order model, 'lnC' was plotted as a function of 't' and for 2nd order model, '1/C' was plotted as a function of 't', where C is the metal ion concentration, and t is the time (Fig. 12 A, B). The slope of each model gives the reaction rate 'k'. The correlation coefficient for the 1st order reaction model was found to be higher ($R^2 = 0.85$). Therefore, the nickel leaching kinetics is following a 1st order reaction. The reaction rate for a 1st order reaction model is found to be 0.0077.

3.3. High-temperature roasting

Bioleached residue was roasted at 700 °C for 1 h to burn down the carbon content and liberate residual refractory metals from the matrix. The bioleached residue observed 9.84% weight loss after roasting due to the burning of light hydrocarbons, soft and hard coke (Marafi and Rana, 2018). The physical and chemical properties of the spent catalyst bioleach residue changed post-roasting. The blackish appearance of bioleached residue changed to white (carbon loss). The morphology of roasted bioleach residue is remarkably altered. The flaky needle-like morphology can be seen in SEM micrographs which could be of aluminium silicate backbone (Fig. 10C). Roasting liberated the matrix-bound metals to get exposed for the attack of alkaline lixiviant. The presence of the peaks of Mo and Al phases in the XRD of roasted residue confirms the presence of residual metal which could have been exposed more due to roasting. Bioleaching in the prior step has leached up to 70% molybdenum which might be due to proton leaching as well as ferric leaching of oxidic and sulphidic phases. The refractory Mo phases which were less accessible for the H^+ or Fe^{3+} attack during bioleaching remained in the bioleached residue; underwent oxidation during roasting and evolution of sulphur dioxide gas took place (equation (13)).

$$MoS_2 + 3.5O_2 \rightarrow MoO_3 + 2SO_2 \quad (13)$$

XRF data suggest that almost 58% of the total sulphur content in the feed material was oxidized during bioleaching. Only, remaining 42% of the sulphur in bioleached residue accounted for SO_2 emission during roasting. According to XRF, 3.85 g sulphur in the bioleached residue was subjected to roasting which would account for 7.71 g SO_2 emission. Had bioleaching not been done before roasting, 22 g SO_2 emission would have occurred. Therefore, bioleaching before roasting has lessened the harmful SO_2 emission into the atmosphere as proposed. The XRF data revealed that several metals had been concentrated in the roasted bioleached residue viz. molybdenum (23.05%), copper (13%), titanium (8%), rubidium (48.25%) and strontium (21.84%). Lead (Pb), which was not detected in the bioleached residue also got concentrated after roasting. The percentage of several elements like aluminium,

Table 2
Elemental composition of Bioleach residue.

Bioleach residue	% (w/w)											
	Al	Mo	S	Ni	P	Si	Fe	K	Ca	Ti	Re	Cr
	45.5	13.7	6.88	0.44	3.77	21.1	2.7	3.5	0.98	0.98	0.052	ND
	Cu	**Se**	**Ga**	**Zr**	**Rb**	**Sr**	**Pd**	**Nb**	**As**	**Pb**	**Na**	
	0.013	0.022	0.017	0.033	0.015	0.013	0.296	0.016	0.015	ND	ND	

Table 3
Elemental composition of Roasted residue.

Roasted residue	% (w/w)											
	Al	Mo	S	Ni	P	Si	Fe	K	Ca	Ti	Re	Cr
	47.1	18.7	ND	0.41	3.38	22	2.71	3.47	0.887	1.17	ND	ND
	Cu	**Se**	**Ga**	**Zr**	**Rb**	**Sr**	**Pd**	**Nb**	**As**	**Pb**	**Na**	
	0.0164	0.015	0.0159	0.0339	0.025	0.0173	ND	ND	ND	0.0346	ND	

nickel, silica, potassium, calcium, gallium and zirconium does not change much post-roasting. Thus, the mineralogical (XRD) and chemical analysis (XRF/SEM-EDAX) of the roasted bioleached residue attribute to the elimination of deposited carbon and exposure of embedded metals resulting in efficient mass transfer and better interaction between alkaline leachate and metal oxides in the next step.

3.4. Alkaline Na_2CO_3–$NaHCO_3$ leaching–

The alkaline leaching system with CO_3^{2-}- HCO_3^- in 2:1 ratio increased the leaching yield of molybdenum by 21%. Mo was leached up to 92% post alkaline leaching treatment. The carbonate-bicarbonate leaching system is highly selective for Mo and V oxoanions (equations (14) and (15)). Also, for avoiding re-precipitation and maximum dissolution of molybdate species, the NaOH produced during the reaction is neutralized by $NaHCO_3$ (Equation (16)). Sodium hydroxide is not as selective as Na_2CO_3 for Mo, and it may dissolve some Al as well in the form of sodium aluminate which will lead to decrease in leaching efficiency of Mo due to less availability of the leachate for Mo dissolution (Al-Sheeha et al., 2013).

$$MoO_3 + 2Na_2CO_3 + H_2O \rightarrow Na_2MoO_4 + 2NaOH + 2CO_2 \quad (14)$$

$$2MoO_3 + 2Na_2CO_3 \rightarrow 2Na_2MoO_4 + 2CO_2 \quad (15)$$

$$NaHCO_3 + NaOH \rightarrow Na_2CO_3 + H_2O \quad (16)$$

Many researchers have also reported good recovery of molybdenum with ammonium salts (Marafi and Rana, 2018; Pradhan et al., 2013; Srichandan et al., 2015). The chemical cost for the alkaline leaching (70 g/L Na_2CO_3) in the present study is estimated to be $4000 for 700 Kg ($Na_2CO_3$)/ton of roasted bioleached spent catalyst which is quite cost-effective as compared to other chemicals which reported good Mo recovery in many studies like 0.5–1M $(NH_4)_2CO_3$ will cost ~ $5260-10000 for 400-900 Kg $(NH_4)_2CO_3$/ton of bioleached–roasted spent catalyst. This cost will increase if the spent catalyst is directly subjected to roasting and alkaline leaching without bioleaching. Due to the attack of alkaline lixiviant, the alkaline leached residue surfaces appear cratered and rough in the SEM micrographs (Fig. 10D). No peaks of molybdenum were observed in the XRD of alkaline leached residue (Fig. 1). High peaks of aluminium silicates, quartz, titanium phases which could not be dissolved by the alkaline leachate were observed in XRD.

Along with good recovery of Mo, other elements like titanium, zirconium, strontium, and rubidium were leached up to 16.33%, 23.8%, 8.794%, and 9.14% respectively (Fig. 12). The recovery (%) of copper was increased by 1.95% only. Some critical elements like rhenium, selenium, and lead present in the bioleached residue were not found in the XRF analysis of alkaline leached residue. According to XRF, several elements also got concentrated during chemical leaching such as chromium which was undetected in bioleached residue got concentrated by 0.49% in the alkaline leached residue. Aluminium also got concentrated by 4%. Rare earth metal like gallium and toxic element like arsenic were also concentrated by 26.41% and 0.125% respectively. More interestingly, precious metal palladium which concentrated by 19% in the bioleached residue was further concentrated by 1.83% after alkaline leaching can be targeted for recovery by employing a suitable and cost-effective treatment.

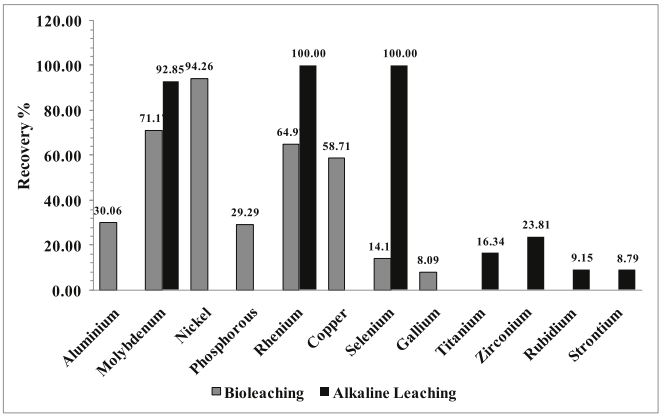

Fig. 9. Comparative bar graph representing leaching yield (%) of metals.

Table 5
Experiment summary of the bioleaching –roasting-alkali leaching of petroleum refinery spent catalyst.

	Bioleaching (Fe &S Oxidizers, 6 Days)	Roasting (700°C, 1 h)	Alkali Leaching (Na_2CO_3:$NaCO_3$- 2:1, 6 h)
Feed weight, g	100	56.06	10
Residue weight, g	67.33	50.54	10.05
Weight loss, %	32.67	9.846	–
Acid Consumption, kg conc. H_2SO_4/ton spent catalyst	212.27	–	–

4. Conclusion

The integrated approach for leaching nickel and molybdenum from spent petroleum catalyst includes 1- bioleaching, 2- roasting and 3- alkaline leaching. In the first step, 94% Ni and 71% Mo were leached out from the feed material. Lesser acid consumption (212 Kg H_2SO_4/ton of Spent Catalyst), high viable cell count (3×10^7 cells/ml) and good ferrous-ferric redox couple ensured the efficiency of the bioleaching process. Nickel bioleaching followed intermediate leaching kinetics due to similar coefficients of correlation (R^2) and is limited by both lixiviant

Table 4
Elemental composition of alkaline leach residue.

Alkaline leach residue	% (w/w)											
	Al	Mo	S	Ni	P	Si	Fe	K	Ca	Ti	Re	Cr
	49.1	1.33	ND	0.55	4.09	33.2	3.26	3.04	1.03	0.97	ND	0.049
	Cu	**Se**	**Ga**	**Zr**	**Rb**	**Sr**	**Pd**	**Nb**	**As**	**Pb**	**Na**	
	0.016	ND	0.02	0.026	0.023	0.016	0.183	ND	0.013	ND	3.02	

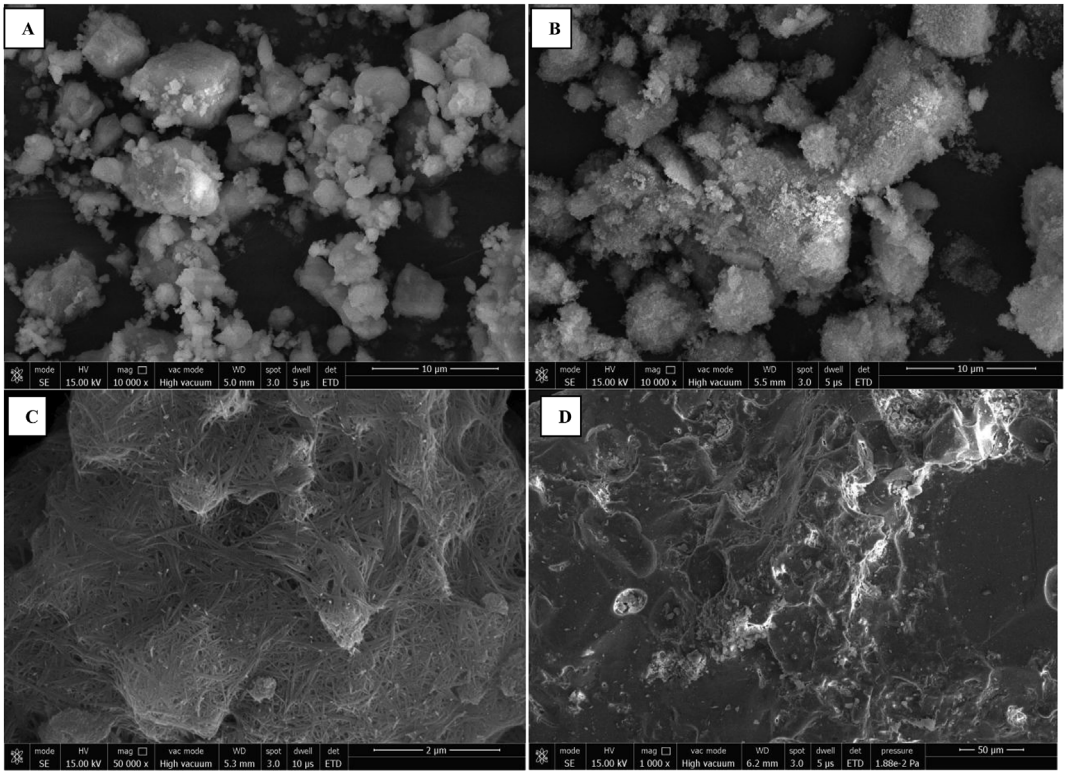

Fig. 10. SEM images showing changes in the morphology of spent catalyst A-Feed, B- Bioleached residue, C- Roasted bioleached residue, D-Alkaline leached residue.

(ferric ion and H^+) and a diffusion layer. Along with Ni and Mo, metals like Re (65%), Cu (58%), Cr (ND), Al (30%), Se (14%), Ga (8%) were also leached during bioleaching. The bioleaching process oxidized around 58% of sulphur content. In the second step, the roasting of the bioleached residue was done for 1 h at 700 °C to burn down coke and liberate residual metal content by minimizing the harmful effect of SO_2 gas emission. Several metals including Mo (23%), Cu (13%), Rb (48%), Sr (22%) and Pb (1.7%) were concentrated after roasting. In the third step, leaching with sodium carbonate-bicarbonate alkaline solution (2:1) was done for 6 h at high temperature. The leaching yield of Mo was increased by 21%. Other elements like Se, Re, and Pb were not detected in the alkaline leached residue whereas recoveries of Ti (16%), Zr (24%), Rb (9%) and Sr (8%) were also increased. Palladium was concentrated by 19% which can be further recovered by additionally employing a cost-effective process. Arsenic (0.001 g) present in traces was also concentrated. Therefore, combining the three leaching tools viz. bioleaching, pyrometallurgy, and hydrometallurgy for environment-friendly and economical extraction of Ni and Mo which were the prime focus of this study proved to be an effective strategy.

Acknowledgments

The authors are thankful to the Department of Science and Technology, Govt. India for funding the research from DST-SERB for

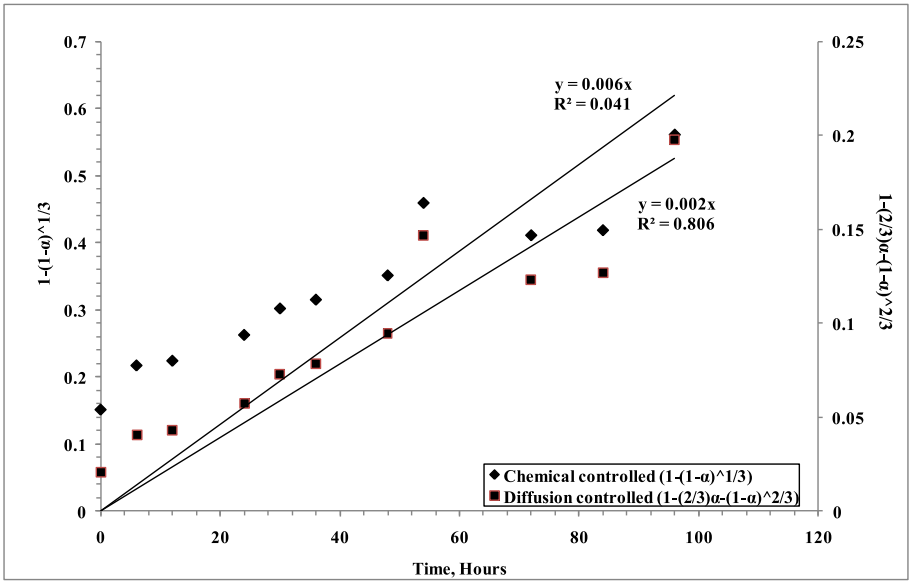

Fig. 11. Chemically and diffusion controlled leaching kinetics study of the bioleaching experiment.

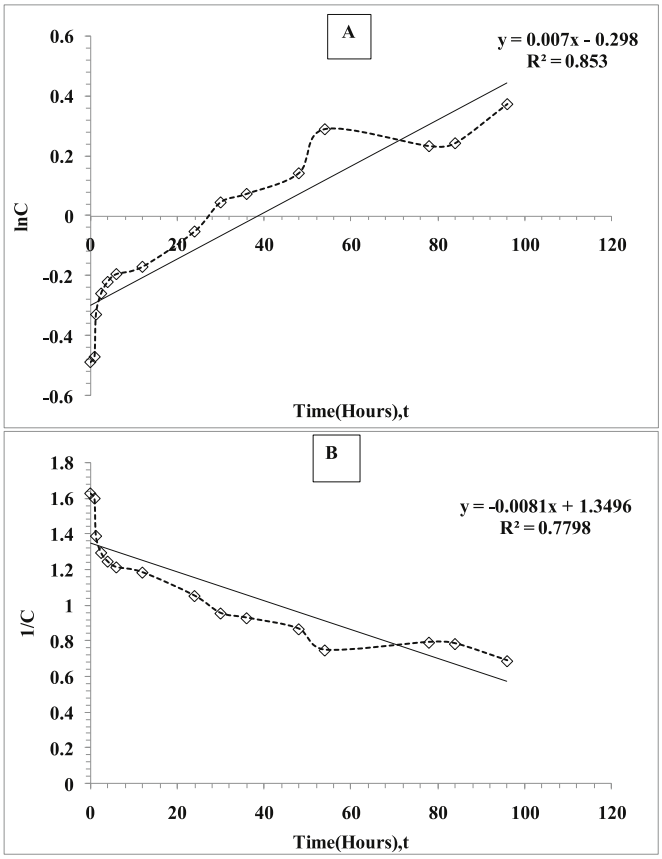

Fig. 12. Reaction order study of nickel leaching reaction.

Young Scientist YSS/2014/000895 and the DST-Inspire Fellowship for the work. Authors would also like to thank UGC and CURAJ for the fellowship. Authors wish to thank Indian Oil Corporation Limited (IOCL) Refinery, Mathura, Uttar Pradesh, India for providing the spent catalyst samples for the research work. Authors would also like to gratefully acknowledge Dr. Ranjan Kumar Dwari, Mineral Processing Technology Department, CSIR-IMMT for his coordination and support for the work. Authors would like to thank Dr. Prakash Chandra Sahoo, IOCL, Faridabad for his coordination and support in XRF analysis, Material Research Center, MNIT, Jaipur, Rajasthan for SEM studies and Department of Physics, CURAJ for the support in XRD analysis of the samples.

References

Akcil, A., Vegliò, F., Ferella, F., Okudan, M.D., Tuncuk, A., 2015. A review of metal recovery from spent petroleum catalysts and ash. Waste Manag. 45.

Al-Sheeha, H., Marafi, M., Raghavan, V., Rana, M.S., 2013. Recycling and recovery routes for spent hydroprocessing catalyst waste. Ind. Eng. Chem. Res. 52, 12794–12801. https://doi.org/10.1021/ie4019148.

Ding, Y., Zhang, S., Liu, B., Zheng, H., Chang, C., Ekberg, C., 2019. Recovery of precious metals from electronic waste and spent catalysts: a review. Resour. Conserv. Recycl. 141, 284–298.

Franzmann, P.D., Haddad, C.M., Hawkes, R.B., Robertson, W.J., Plumb, J.J., 2005. Effects of temperature on the rates of iron and sulfur oxidation by selected bioleaching Bacteria and Archaea: application of the Ratkowsky equation. Miner. Eng. 18, 1304–1314.

He, D., Feng, Q., Zhang, G., Ou, L., Lu, Y., Shao, Y., 2007. The study on leaching vanadium from stone coal with alkali [J]. Nonferrous Met. (Extractive Metall. 4, 17–19.

Kim, D.-J., Pradhan, D., Ahn, J.-G., Lee, S.-W., 2010. LEnhancement of metals dissolution from spent refinery catalysts using adapted bacteria culture—effects of pH and Fe (II). Hydrometallurgy 103, 136–143.

Kinnunen, P.H.-M., Puhakka, J.A., 2005. High-rate iron oxidation at below pH 1 and at elevated iron and copper concentrations by a Leptospirillum ferriphilum dominated biofilm. Process Biochem. 40, 3536–3541.

Kolmert, Å., Wikström, P., Hallberg, K.B., 2000. A fast and simple turbidimetric method for the determination of sulfate in sulfate-reducing bacterial cultures. J. Microbiol. Methods 41, 179–184.

Leahy, M.J., Schwarz, M.P., 2009. Modelling jarosite precipitation in isothermal chalcopyrite bioleaching columns. Hydrometallurgy 98, 181–191.

Levenspiel, O., 1999. Chemical reaction engineering. Ind. Eng. Chem. Res. 38, 4140–4143.

Longa, S., Fenga, Q., Zhanga, G., Heb, D., 2014. Recovery of vanadium from alkaline leaching solution from roasted stone coal. Sci. Asia 40, 69.

Marafi, M., Rana, M.S., 2018. Metal leaching from refinery waste hydroprocessing catalyst. J. Environ. Sci. Heal. Part A 53, 951–959.

Marafi, M., Rana, M.S., 2017. Refining waste spent hydroprocessing catalyst and their metal recovery. World Acad. Sci. Eng. Technol. 11, 893–897.

Marafi, M., Stanislaus, A., 2011. Alumina from reprocessing of spent hydroprocessing catalyst. Catal. Today 178, 117–123. https://doi.org/10.1016/j.cattod.2011.07.001.

Marafi, M., Stanislaus, A., 2008. Spent hydroprocessing catalyst management: a review: Part II. Advances in metal recovery and safe disposal methods. Resour. Conserv. Recycl. 53, 1–26.

Mishra, D., Kim, D.J., Ralph, D.E., Ahn, J.G., Rhee, Y.H., 2007. Bioleaching of vanadium rich spent refinery catalysts using sulfur oxidizing lithotrophs. Hydrometallurgy 88, 202–209.

Pathak, A., Srichandan, H., Kim, D.-J., 2014. Fractionation behavior of metals (Al, Ni, V, and Mo) during bioleaching and chemical leaching of spent petroleum refinery catalyst. Water, Air, Soil Pollut. 225, 1893.

Plumb, J.J., Muddle, R., Franzmann, P.D., 2008. Effect of pH on rates of iron and sulfur oxidation by bioleaching organisms. Miner. Eng. 21, 76–82.

Pradhan, D., Mishra, D., Kim, D.J., Ahn, J.G., Chaudhury, G.R., Lee, S.W., 2010. Bioleaching kinetics and multivariate analysis of spent petroleum catalyst dissolution using two acidophiles. J. Hazard Mater. 175, 267–273.

Pradhan, D., Mishra, D., Kim, D.J., Chaudhury, G.R., Lee, S.W., 2009. Dissolution kinetics of spent petroleum catalyst using two different acidophiles. Hydrometallurgy 99, 157–162.

Pradhan, D., Patra, A.K., Kim, D.-J., Chung, H.-S., Lee, S.-W., 2013. A novel sequential process of bioleaching and chemical leaching for dissolving Ni, V, and Mo from spent petroleum refinery catalyst. Hydrometallurgy 131, 114–119.

Sand, W., Gehrke, T., Jozsa, P.-G., Schippers, A., 2001. Bio)chemistry of bacterial leaching—direct vs. indirect bioleaching. Hydrometallurgy 59, 159–175. https://doi.org/10.1016/S0304-386X(00)00180-8.

Silverman, M.P., Lundgren, D.G., 1959. Studies on the chemoautotrophic iron bacterium Ferrobacillus ferrooxidans: I. An improved medium and a harvesting procedure for securing high cell yields. J. Bacteriol. 77, 642.

Srichandan, H., Singh, S., Blight, K., Pathak, A., Kim, D.J., Lee, S., Lee, S.W., 2015. An integrated sequential biological leaching process for enhanced recovery of metals from decoked spent petroleum refinery catalyst: a comparative study. Int. J. Miner. Process. 134. https://doi.org/10.1016/j.minpro.2014.11.002.

Sundkvist, J., Gahan, C.S., Sandström, Å., 2008. Modeling of ferrous iron oxidation by a Leptospirillum ferrooxidans-dominated chemostat culture. Biotechnol. Bioeng. 99, 378–389.

Tan, Y., Wang, Z.-X., Marshall, K.C., 1998. Modeling pH effects on microbial growth: a statistical thermodynamic approach. Biotechnol. Bioeng. 59, 724–731.

Vyas, S., Ting, Y.-P., 2016. Sequential biological process for molybdenum extraction from hydrodesulphurization spent catalyst. Chemosphere 160, 7–12.

Wang, J., Huang, X., Wang, L., Wang, Q., Yan, Y., Zhao, N., Cui, D., Feng, Z., 2017. Kinetics study on the leaching of rare earth and aluminum from FCC catalyst waste slag using hydrochloric acid. Hydrometallurgy 171, 312–319.

Zhao, Z., Guo, M., Zhang, M., 2015. Extraction of molybdenum and vanadium from the spent diesel exhaust catalyst by ammonia leaching method. J. Hazard Mater. 286, 402–409. https://doi.org/10.1016/j.jhazmat.2014.12.063.